

# Combining one- and two-dimensional signal recognition approaches to off-line signature verification

Siyuan Chen and Sargur Srihari

Center of Excellence for Document Analysis and Recognition (CEDAR), University at Buffalo,  
State University of New York, Buffalo, 14228 USA

## ABSTRACT

A signature verification method that combines recognition methods of one-dimensional signals, e.g., speech and on-line handwriting, and two-dimensional images, e.g., holistic word recognition in OCR and off-line handwriting is described. In the one-dimensional approach, a sequence of data is obtained by tracing the exterior contour of the signature which allows the application of string-matching algorithms. The upper and lower contours of the signature are first determined by ignoring small gaps between signature components. The contours are combined into a single sequence so as to define a pseudo-writing path. To match two signatures a non-linear normalization method, *viz.*, dynamic time warping, is applied to segment them into curves. Shape descriptors based on Zernike moments are extracted as features from each segment. A harmonic distance is used for measuring signature similarity. The two-dimensional approach is based on using features describing the word-shape. When the two methods are combined, the overall performance is significantly better than either method alone. With a database of 1320 genuines and 1320 forgeries the combination method has an accuracy of 90%.

## 1. INTRODUCTION

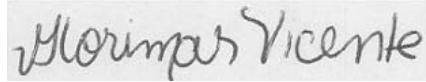
The task of signature verification is to learn from a set of known signatures so that one can determine whether a signature of unknown origin belongs to that set. This task is of relevance to complex document processing, forensics, biometrics, etc.

While *on-line*, or dynamic, signature verification has a significant body of literature<sup>1</sup>—with reported accuracies of over 95%<sup>2</sup>—the topic of *off-line*, or static, signature verification is more difficult and continues to be of research interest. The differences arise due to the two-dimensional nature of the off-line signature signal as opposed to the one-dimensional temporal signal in the on-line case. One model for the off-line case is based on tracking histogram variations of signatures by dynamic timing warping (DTW), building statistics and based on a skeleton of a signature stroke.<sup>3</sup> Another off-line method approaches the problem from a multi-resolution viewpoint based on the wavelet model.<sup>4</sup> Graphometric features used by questioned document examiners were implemented and achieved good performance.<sup>5</sup> A previous method developed at CEDAR for handwritten word recognition—one that captures word shape using gradient, structural and concavity (or GSC) features—performed well in the signature verification task.<sup>6</sup> However, no previous research focuses on characteristics of stroke shape that have proved to be most reliable feature in on-line systems.<sup>2</sup> Once the off-line signature is described by an ordered series of points, shape descriptors—used with success in image recognition—can be used as features<sup>7,8</sup> and approaches for on-line systems can be utilized. Aspects of the method described here are also given in.<sup>9</sup>

## 2. IMAGE PRE-PROCESSING

1. *Binarization*: Each signature was scanned at a 300 dpi grayscale. Then the grayscale images were converted to binary images by Otsu's thresholding method (Fig. 1).

2. *Broken stroke connection (Adaptive image enhancement)*: The image may be broken due to several reasons: imperfect binarization, disconnect between pen tip and paper surface, etc. Binary images are usually enhanced using closing and opening operations based on fixed structuring elements. For signature images, however, closing and opening will result in deformations like thickening—which may destroy smoothness of stroke shape. A  $7 \times 7$  window is placed on each black pixel with the center mapped with the mid-point of the stroke. Depending on the left- and right-most coordinates of black pixel in each line of the window, appropriate background pixels are converted into foreground pixels to connect the isolated foreground pixel. Due to the window size of  $7 \times 7$  even



(a)



(b)



(c)

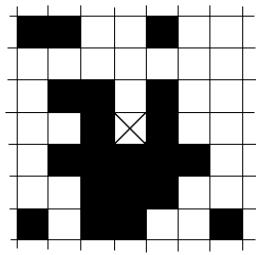
**Figure 1.** Image pre-processing: (a) original grayscale image, (b) binary image after thresholding, (c) image after enhancement using method shown in Fig 2.

foreground pixels separated by chessboard distance of 2 can be connected (Fig. 2). Adaptive stroke connection preserves details of the original stroke and smoothes edges as well (Fig. 1). This method is a modification of .<sup>11</sup>

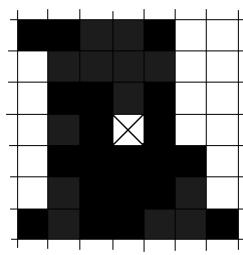
**Algorithm for stroke connection:**

```

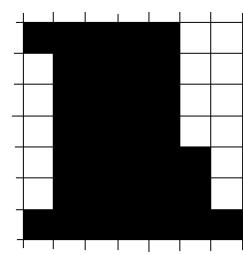
for(i=Top line:bottom line){
    for(j=left column:right column){
        if(the current pixel (i,j) is foreground pixel and unprocessed){
            for(any line in the 7 × 7 region centered in it){
                find the left most and right most foreground pixel;
                convert the pixels between them into foreground;
                mark the pure background line;
            }
            for(p=top non-background line:bottom non-background line){
                find the next non-background line q;
                compute the line function L connecting the centers of left most
                pixels of line p and q;
                compute the line function R connecting their right most pixels;
                for(every background line bween p and q){
                    find the pixels closest to line L and line R respectively;
                    convert the pixels between them;
                }
            }
            mark the central pixel as processed;
        }
    }
}
}
```



(a)



(b)



(c)

**Figure 2.** Broken stroke connection. (a) a  $7 \times 7$  region to be repaired, (b) enhancement procedure, (c) The region after enhancement

### 3. ONE-DIMENSIONAL APPROACH BASED ON CONTOUR TRACING

The idea of stroke characterization led to the new off-line signature verification described here. By combining the exterior contours of the signature image into a single contour, ranking the pixels on the contour in the clockwise order, a pseudo-writing path is constructed. After a simple modification, most algorithms for on-line systems can be used. The approach depends on the construction of a single contour. The ideal contour would be invariant among genuines and discriminative between genuines and forgeries. Even if the structure and shape of a signature are relatively invariant between genuines, differences arise in the number of extracted contours and their positional relationships due to the dynamics of signing, shortcomings of image pre-processing, etc. Since signatures are along a line, the relative positional relation of discrete components along the direction perpendicular to the signature line are invariant between genuines. Imagining the signature components as a linearly arranged jigsaw puzzle, the discrete contour components can be from right to left along the line until they touch. Then a single contour can be extracted. Undoubtedly some information is lost by ignoring interior contours and distances between discrete contours. While previously developed algorithms may also ignore certain characteristics, we only attempt to show the discriminating power of features extracted from the combined contour and the possibility of their being part of a mature verification system. After this step, DTW is used to segment the constructed contour into separated curves and extract Zernike moments<sup>10</sup> from them respectively. (Fig. 3). Both the DTW algorithm and Zernike moments are widely used in pattern recognition. Without discussing the possible utility of many methods developed for on-line systems, performance of the proposed system reaches the level of developed systems, such as ones based on dynamic grid and word-shape features, and leaves a large space for future research.

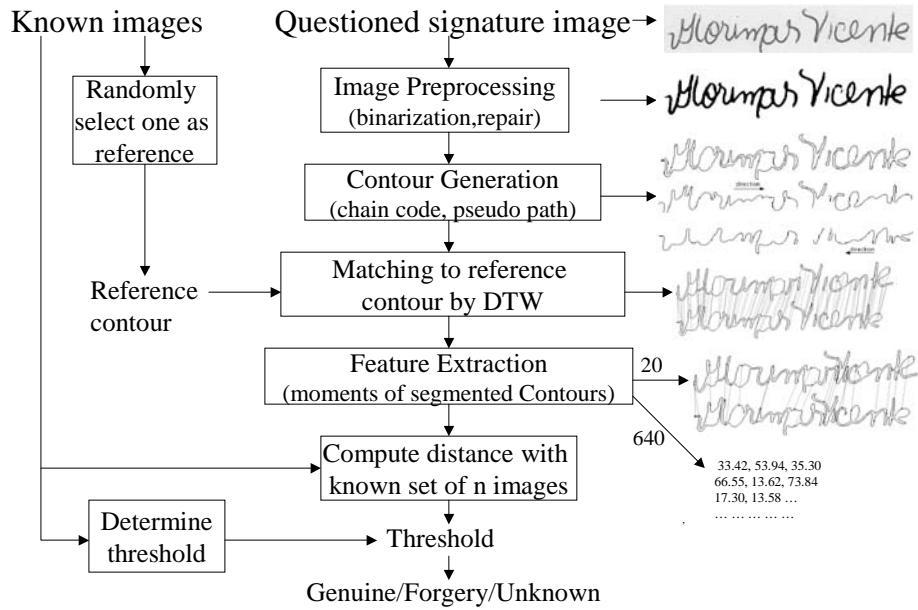


**Figure 3.** Framework of contour-based method

*3. Contour extraction:* Exterior contours are obtained from the binary images by scanning the image left-to-right and top-to-bottom. Contours extracted are shown in Fig. 4 where there are five exterior contours.

The extracted contour pixels are saved in clockwise order. The extracted information includes each pixel's position, slope, and curvature, each contour's length in pixels and contour's frame size (Fig. 6). These values are used in DTW contour matching described in Section 3.2.

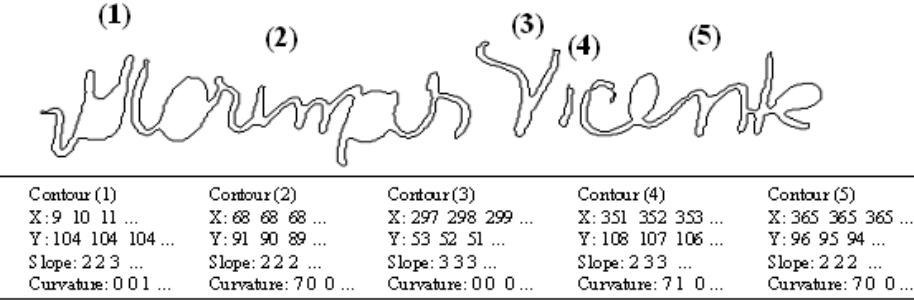


**Figure 4.** Exterior contours of signature. There are 5 disconnected contour components in this signature. And the information about position, slope and curvature of the pixels along each contour is extracted as well.

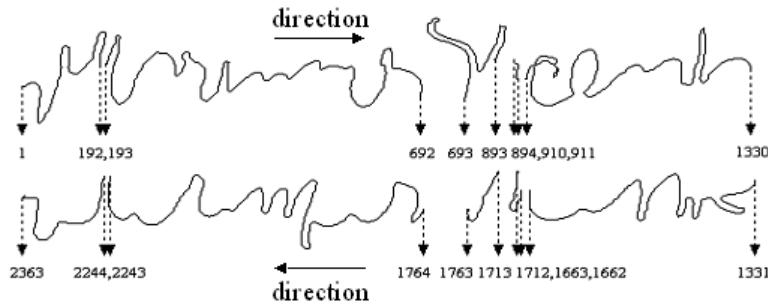


**Figure 5.** Pseudo path construction. The pixels of all the extracted contours are indexed so as to form a pixel sequence.

4. *Noise removal:* Small contours with size less than 50 are ignored. Edge noise due to scanning usually appears as long black lines in the image— which can be recognized by extremely large ratio of contour frame width to length— and removed.

### 3.1. Combining contours of a signature

The goal of this step is to combine all the contours in the image into a single contour, or obtain a unique closed loop. It is possible to achieve a relative steady path for each writer. The starting point of this loop is the first pixel of left most contour. The ending point of this loop is the last pixel of the same contour. To get the loop, each contour is separated into two parts: the upper part and lower part. So the path is to pass the upper parts of all contours from left to right and then pass the lower parts from right to left. The key point is how to separate each contour into two parts: the left cut point is the one closest to the left neighbor contour; similarly, the right cut point is the one *closest* to the right neighbor contour. For the left most contour, the left cut point is the left most pixel. Similarly, for the right most contour, the right cut point is the right most pixel. If a contour has no neighbor contour, the cut points are selected from its left most and right most pixels respectively (Fig. 7).

### 3.2. Matching contours of two signatures

The points along the two contours of the reference and test signature are matched using DTW. For each writer, the combined contour of shortest length is chosen as the reference image and the rest are normalized by DTW with respect to this reference. Use of DTW here differs from its use in speech recognition<sup>12</sup> or in on-line systems. Here the time domain is the index of contour pixel instead of sampling time index. The cost function for DTW is the quadratic average of difference in slope and curvature.

A new set of local constraints and slope weights is designed to meet the need of this application (Fig. 8).

The algorithm is given as follows:

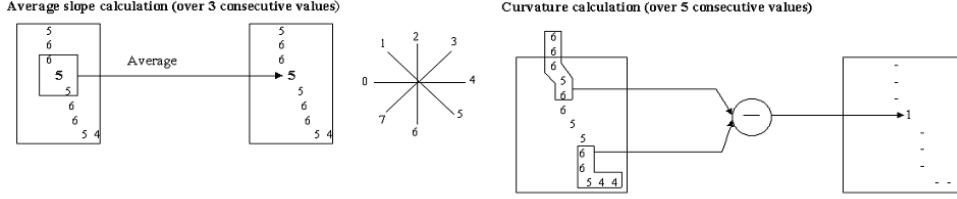


**Figure 6.** Slope and curvature computation.



**Figure 7.** Contour alignment and segmentation. (a) The contours of different signature are alignment by DTW, (b) The contour sequences are divided into 20 segments consequently.

- Initialization:  $D_A(0, 0) = d(0, 0)$ . where

$$d(i_x, i_y) = [f_s^2(\text{slope}(i_x) - \text{slope}(i_y)) + f_c^2(\text{curvature}(i_x), \text{curvature}(i_y))]^{\frac{1}{2}} \quad (1)$$

and

$$f_s(x) = \begin{cases} x & \text{if } x < 5 \\ 8 - x & \text{if } x \geq 5 \end{cases} \quad (2)$$

$$f_c(x_1, x_2) = (x_1 + 3)\%8 + (x_2 + 3)\%8 \quad (3)$$

From (2) and (3) we see that the distance in slope and curvature have been modified to fit the direction quantization.

- Recursion: For  $0 \leq T_x - 1, 0 \leq T_y - 1$  such that  $i_x$  and  $i_y$  stay within the allowable grid,

$$\frac{\phi_x(k)}{Q_{max}} \leq \phi_y(k) \leq \frac{\phi_x(k)}{Q_{min}} \quad (4)$$

$$T_y - 1 + \frac{\phi_x(k) - T_x + 1}{Q_{min}} \leq \phi_y(k) \leq T_y - 1 + \frac{\phi_x(k) - T_x + 1}{Q_{max}} \quad (5)$$

Compute

$$D_A(i_x, i_y) = \min_{i'_x, i'_y} [D_A(i'_x, i'_y) + \xi((i'_x, i'_y), (i_x, i_y))] \quad (6)$$

$$\xi((i'_x, i'_y), (i_x, i_y)) = \sum_{l=0}^{L_s} d(\phi_x(T' - l), \phi_y(T' - l)) \times m(T' - l) \quad (7)$$

where  $L_s$  is the number of moves from  $(i'_x, i'_y)$  to  $(i_x, i_y)$ ,  $m$  is slope weight.

- Termination:

$$d(X, Y) = \frac{D_A(T_x - 1, T_y - 1)}{M_\phi} \quad (8)$$

where  $M_\phi = T_x + T_y$

Note:  $x$  and  $y$  refer to the index of test image and reference image respectively.

$\phi_x(k), \phi_y(k)$  — the warping function

$Q_{max}, Q_{min}$  — the parameters to specify the maximum and minimum expansion of warping

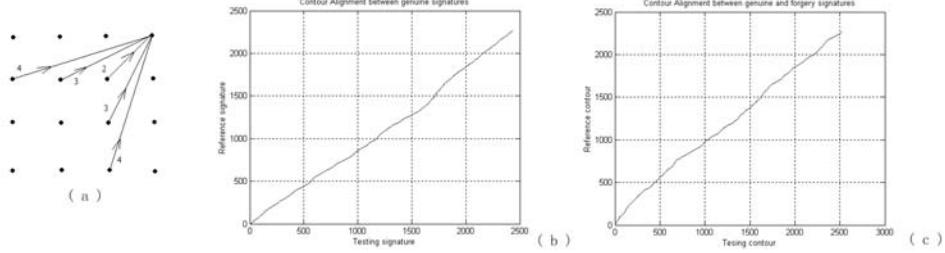


**Figure 8.** DTW path: (a) local constraints and slope weights, (b) genuine-genuine contour alignment, and (c) genuine-forgery contour alignment.

### 3.3. Feature extraction

The signature contour is segmented into a fixed number,  $k$ , of small curves linearly so that shape features can be separately computed for each curve. Corresponding parts of the contour are segmented in the pair of signatures to be matched based on the result of DTW contour matching. Experimentation led to a choice of  $k = 20$ .

Features are extracted for each segment by using Zernike moments. They are based on a set of complex polynomials which form a complete orthogonal set over the interior of the unit circle, i.e.  $x^2 + y^2 = 1$ .<sup>10</sup> These polynomials,  $V_{nm}(x, y)$ , have the form<sup>7</sup>:

$$V_{nm}(x, y) = V_{nm}(\rho, \theta) = R_{nm}(\rho) \exp(jm\theta) \quad (9)$$

where  $n$  are positive integers or zero and  $m$  are integers subject to  $|m| < n, n - |m| \in \text{even}$ ,  $\rho$  is the distance between  $(x, y)$  and the origin,  $\theta$  is the angle between the vector formed above and the x-axis in counter-clockwise direction, and

$$R_{nm}(\rho) = \sum_{s=0}^{(n-|m|)/2} (-1)^s \frac{(n-s)!}{s!(\frac{n+|m|}{2}-s)!(\frac{n-|m|}{2}-s)!} \rho^{n-2s}. \quad (10)$$

The Zernike moment with order  $n$  and repetition  $m$  for a digital image  $f(x, y)$  is defined as:

$$A_{nm} = \frac{n+1}{\pi} \sum_x \sum_y f(x, y) V_{nm}^*(\rho, \theta) \quad x^2 + y^2 \leq 1 \quad (11)$$

Here  $f(x, y)$  is binary-valued, i.e. 0 or 1.

If the image is rotated clockwise by angle  $\alpha$ , then the Zernike moment of the rotated image is<sup>7</sup>

$$A_{nm}^r = A_{nm} \exp(-jm\alpha). \quad (12)$$

From (12) it follows that the magnitude of the Zernike moment records shape information and the complex angle records rotation angle with respect to the origin. Magnitude is a rotation invariant feature that represents the shape of the curve. With signatures the rotation angle of the segmented curve is a significant characteristic. Thus both magnitude and angle are used as features.

For each segment, the starting point is chosen as the co-ordinate origin. Sixteen Zernike moments, up to order 6 as shown in Table 1, are extracted. Thus  $16 \times 2 \times 20 = 640$  Zernike feature values are extracted from the signature.

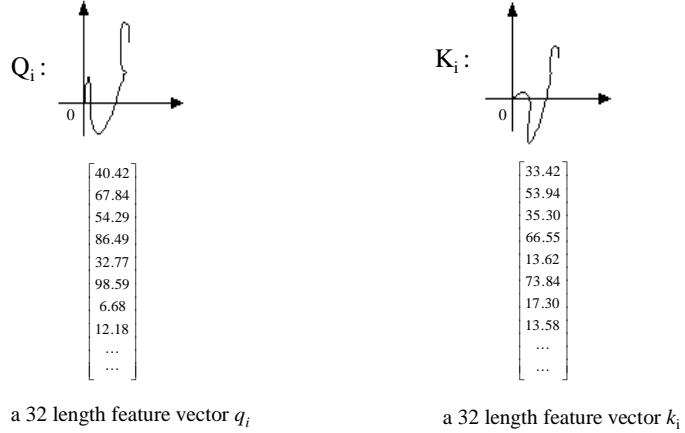
**Table 1.** Selected Zernike Moments

ORDER	MOMENTS	NO.
0	$A_{00}$	1
1	$A_{11}$	1
2	$A_{20}, A_{22}$	2
3	$A_{31}, A_{33}$	2
4	$A_{40}, A_{42}, A_{44}$	3
5	$A_{51}, A_{53}, A_{55}$	3
6	$A_{60}, A_{62}, A_{64}, A_{66}$	4

### 3.4. Measuring signature similarity

Due to the dynamic characteristic of the signing process, the harmonic mean dissimilarity measure <sup>2</sup> is applied to measure dissimilarity between the extracted feature vectors. Different from the Euclidean distance, harmonic mean dissimilarity is the reciprocal of summation of reciprocals of Euclidean distance of feature vector of each segment, i.e.,  $D = \frac{1}{\sum_i^{\frac{1}{d_i}}}$ , where  $d_i$  denotes the Euclidean distance between contour segments with index  $i$ .

(Fig. 9). Thus if specific segments are highly similar then overall dissimilarity will be low, which matches the fact that in cursive writing people always turn back to their own writing style for some parts even if the writing process is dynamic. ((Given a questioned signature, its distance from every training signature is computed and their average is compared with a prefixed threshold  $t$ . The input signature is labeled genuine when its average distance to the training images is less than  $t$ . Otherwise it is labeled a forgery.))



$$\text{Harmonic distance between questioned and known signatures : } D(Q, K) = \frac{1}{\sum_{i=1}^{20} \frac{1}{d_i}}$$

$$\text{Where } d_i \text{ is the Euclidean distance between the ith segment of signatures } d_i = \sqrt{\sum_{j=1}^{32} (q_{ij} - k_{ij})^2}$$

**Figure 9.** Segment distance computation: Euclidean distances between corresponding 32-dimensional vectors are averaged over 20 segments using their harmonic mean.

## 4. TWO-DIMENSIONAL METHOD BASED ON WORD SHAPE

The Gradient, Structural and Concavity (GSC) algorithm measures the image characteristics at different scale: local, intermediate, and large. The Gradient features measure edge curvature in the neighbor of a pixel. The

Structural features measure short stroke types which span several pixels, and the Concavity features measure certain hole types which can span across the image. For each type of feature, a histogram is computed first and a binary bit, 0 for negative and 1 for positive, is decided for that feature. Cropping the image into  $4 \times 8$  small regions, the GSC features are computed independently for each region and consequently combined into a 1024 binary feature vector. (Fig. 10). See <sup>13</sup> for the detailed description.

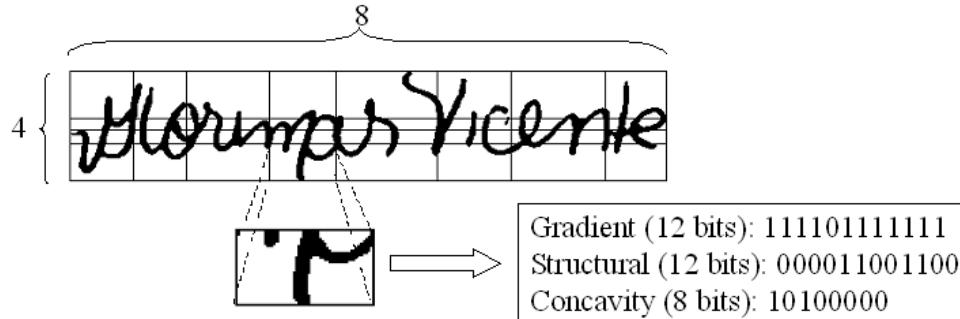


**Figure 10.** A  $4 \times 8$  grid is placed on the image according to histograms along x and y axis respectively. The GSC feature is extracted for each sub-grid and constructed into a 1024 binary feature vector.

The similarity of two images based on GSC feature is measured as:  $score = \frac{0.5 \times C_{00} + C_{11}}{1024}$ . Where  $C_{00}$  is the number of bits where both the images have a 0, similarly,  $C_{11}$  is the number of bits where both the images have a 1.  $C_{00}$  is weighted by 0.5 because the fact that both the images miss the same feature is not as important as the fact that both of them have that feature.

Using the same verification method as Zernike model, the performance of GSC method is compared with Zernike method. (Fig. 12).

#### 4.1. Performance

Unfortunately there is no common data set in the area of signature verification. Thus it is difficult to compare the performance of developed systems so far. For the purpose of evaluating the method a testbed of signatures from 55 volunteers with different cultural backgrounds was used. Each provided 24 signatures taken 20 minutes apart to reduce correlations between signatures due to writer physical status. Some of them simulated the signatures of 3 people, 8 times each, thereby creating 1320 genuines and 1320 forgeries.

For each writer, 16 genuines were randomly selected as training samples and the remaining 8 genuines together with the 24 forgeries were used as testing samples. Before testing, distances between every pair of images, i.e.,  $(16 \times 15 \div 2 = 120)$  cases were computed. Using verification threshold as parameter, the so called error trade-off curve, which is the curve of Type I error(False reject rate or FRR) as the function of Type II error(False accept rate or FAR), is plotted. The circled point is where the false reject rate is equal to false reject rate. It is the well known equal error rate, a number to evaluate the performance of verification algorithm. (Fig. 12).

**Table 2.** Accuracy (55 writers/32 signatures each) with no rejection

SYSTEM	1-FAR	1-FRR	ACCURACY
Zernike moments	83.7	83.4	83.6
Word shape(GSC)	80.5	77.55	78.5
Combined method	90.2	90.0	90.1

	Norman Vicente			
Melissa N. Daniels				

(a)

	Norman Vicente			
Melissa N. Daniels				

(b)

**Figure 11.** Sample genuines and forgeries used in training and testing: (a) sample genuines, and (b) corresponding sample forgeries.

## 5. COMBINATION WITH WORD SHAPE METHOD

The proposed method performs better than the word shape (GSC) approach<sup>6</sup> whose performance is shown in the second row of Table 2– a 5 % increase in accuracy. Although Zernike method has a higher accuracy compared with GSC method, the signatures being mis-verified by them are not necessarily overlapped. And this fact motivates the combined signature verification. Here a simple and efficient combined model is proposed:  $Score = \alpha \times S_{zernike} + \beta \times S_{gsc}$ . Where  $\alpha$  and  $\beta$  are weights for feature of Zernike and GSC model respectively, which are set to achieve a global optimum performance over the dataset,  $S_{zernike}$  and  $S_{gsc}$  are feature scores from Zernike and GSC models, both of them have been normalized to have a range from 0 to 1. From the experimental result, the accuracy of combined model is over 90%.

## 6. CONCLUSION

A signature verification method based on obtaining an exterior contour of the image and features based on Zernicke moments has been described. The method demonstrates strong invariance among genuines, which validates the pseudo-path construction method and the Zernike shape descriptor. When combined with a word shape based approach higher accuracy is obtained thereby demonstrating complementarity of approaches.

## Acknowledgement

This project was supported in part by Grant Number 2004-IJ-CX-K050 awarded by the National Institute of Justice, Office of Justice Programs, US Department of Justice. Points of view in this document are those of the authors and do not necessarily represent the official position or policies of the US Department of Justice.

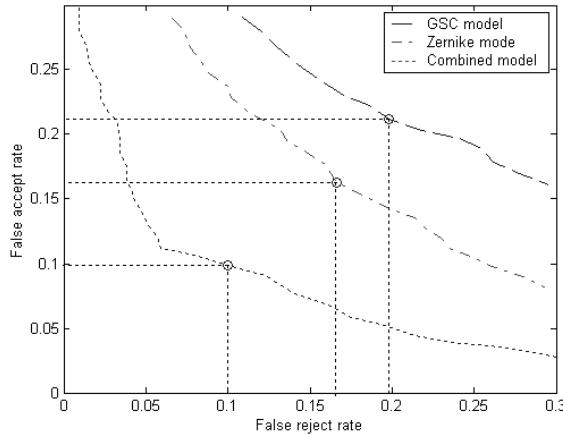


**Figure 12.** False Accept Rate (FAR) versus False Reject Rate (FRR) of three signature verification methods. The combined method has significantly lower error rate than either method alone.

## REFERENCES

1. R. Plamondon and G. Lorette, "Automatic signature verification and writer identification- The state of art", *Pattern Recog.* 22(2), 1989, 107-131.
2. V. S. Nalwa, "Automatic On-Line Signature Verification", *Proc. IEEE*, Vol. 85, No. 2, February 1997.
3. B. Fang, C. H. Leung et al, "Offline-signature verification by the tracking of feature and stroke positions", *Pattern Recog.* 36(2003) 91-101.
4. P. S. Deng, H-Y. Liao, C. Ho and H-R Tyan, "Wavelet-Base Off-Line Handwritten Signature Verification", *Comput. Vision Image Understand.*, Vol. 76, No. 3, December, pp. 173-190,1999.
5. R. Sabourin, "Off-Line Signature Verification: Recent Advances and Perspectives", *BSDIA*, 1997, 84-98.
6. S. N. Srihari, A. Xu, M. K. Kalera, "Learning Strategies and Classification Methods for Offline Signature Verification", *Proc. IWFHR-9*, Tokyo, 2004.
7. A. Khotanzad and Y. Hong, "Invariant Image Recognition by Zernike Moments", *IEEE Trans. Pattern Anal. Mach. Intel.*, Vol. 12, No. 5, May 1990.
8. D. Shen, Horace H. S. Ip, "Discriminative wavelet shape descriptors for recognition of 2-D patterns", *Pattern Recog.* 32 (1999) 151-165.
9. S. Chen and S. N. Srihari, "Use of Exterior Contours and Shape Features in Off-line Signature Verification", *Proc. Int. Conf. on Document Analysis and Recognition(ICDAR-05)*, Seoul, Korea, October 2005
10. F. Zernike, *Physica*, vol. 1, p.689,1934.
11. Z. Shi and V. Govindaraju, "Character Image Enhancement Using Selective Region Growing", *Pattern Recog. Lett.*, Elsevier, 17: 523-527, 1996.
12. L. Rabiner B-H. Juang, *Fundamentals of Speech Recognition*, Prentice Hall.
13. J. T. Favata and G. Srikantan, "A Multiple Feature/Resolution Approach to Hand printed Digit and Character Recognition", *Int. J. Imaging Sys. Tech.* Wiley, 7(4): 304 - 311, 1996.